16th European Signal Processing Conference (EUSIPCO 2008), Lausanne, Switzerland, August 25-29, 2008, copyright by EURASIP

A NEW CFAR DETECTOR IN GAMMA-DISTRIBUTED NONHOMOGENEOUS BACKGROUNDS

Éric Magraner, Nicolas Bertaux, and Philippe Réfrégier

Physics and Image Processing Group, Fresnel Institute, UMR CNRS 6133
École Centrale de Marseille, Université Paul Cézanne
Domaine Universitaire de Saint-Jérôme, 13 397 Marseille Cedex 20, France
phone: + (33)4 91 28 80 78, fax: + (33)4 91 28 80 67
email: firstname.lastname@fresnel.fr, web: www.fresnel.fr/phyti

ABSTRACT

Detecting targets in nonhomogeneous backgrounds is a difficult task, particularly if the detection processor must respect a Constant False Alarm Rate (CFAR). In this article, a novel approach is developed for the detection of punctual targets embedded in nonhomogeneous gamma-distributed backgrounds. The well-known CA-CFAR (Cell-Averaging CFAR) processor is generalized to nonhomogeneous backgrounds through a new CFAR thresholding method. This new CFAR thresholding method allows one the design of new CFAR processors that use other background estimators than the arithmetic mean. A new CFAR processor (Q-CFAR) adapted to nonhomogeneous backgrounds is designed, the improvement of the detection performance, and more particularly the improvement of the false alarm regulation obtained with the proposed CFAR processor is shown with Monte-Carlo experiments.

1. INTRODUCTION

Detection of targets embedded in nonhomogeneous gamma-distributed backgrounds is of interest in different applications such as: RADAR, medical diagnosis. Moreover it is commonly required to control the false alarm[1] number, *i.e.* the detection processor must be a Constant False Alarm Rate processor. However, the regulation of the false alarm rate in nonhomogeneous background is a challenging issue.

In this communication, the detection of an unknown number of punctual targets at unknown locations in an image $\boldsymbol{X}$ is investigated. In homogeneous gamma-distributed backgrounds (and Swerling I target model [1]), Gandhi and Kassam proved the optimality of the CA-CFAR processor [2, 3]. Let p be a pixel of $\boldsymbol{X}$ with coordinates (i_p, j_p) and n be the pixel under test. The problem is to decide if whether the pixel under test n is a target (H_1) or not (H_0). The CA-CFAR processor introduced in [2] uses the following detection test:

$$\frac{X_n}{Z_n} \underset{H_0}{\overset{H_1}{\gtrless}} T. \tag{1}$$

where X_n is the value of the pixel under test n in the image $\boldsymbol{X}$, Z_n is an estimation of the mean value m_n of X_n and T a threshold computed for a given false alarm rate.

Let ω_n be a region in the neighborhood of the pixel n (n is not included in ω_n). The background estimation is generally performed assuming that the region ω_n is homogeneous. Thus the maximum likelihood estimator of the mean Z_n is:

$$Z_n \triangleq \frac{1}{N_n} \sum_{p \in \omega_n} X_p, \;\; N_n \triangleq card(\omega_n). \tag{2}$$

Hereafter, it is assumed that the background $\boldsymbol{m} = E[\boldsymbol{X}]$ is corrupted by a gamma noise with order L, *i.e.* $X_p \sim \mathscr{G}(m_p, L)$ are independent and non-identically distributed gamma random variables (for a homogeneous background, $\forall p \in \omega_n,\ m_p = m_n$).

Using a Swerling I target model [1] with a Signal to Noise Ratio (SNR) S such that $X_n \sim \mathscr{G}(m_n(1+S), L)$ and assuming the homogeneity of ω_n, the detection probability of the CA-CFAR processor is given by [4–6]:

$$\begin{aligned} P_d^{CA-CFAR}(T|S) &\triangleq P(X_n/Z_n > T|H_1) \\ &\triangleq 1 - \mathscr{I}\left(\frac{\frac{T}{N_n(1+S)}}{1+\frac{T}{N_n(1+S)}}, L, N_n L\right), \end{aligned}$$

where $\mathscr{I}(x,a,b)$ is the regularized Beta function defined by:

$$\mathscr{I}(x,a,b) \triangleq \frac{\mathscr{B}_{\mathscr{I}}(x,a,b)}{\mathscr{B}(a,b)},$$

with $\mathscr{B}_{\mathscr{I}}(x,a,b)$ the incomplete Beta function:

$$\mathscr{B}_{\mathscr{I}}(x,a,b) \triangleq \int_0^x u^{a-1}(1-u)^{b-1} du,$$

and the Beta function $\mathscr{B}(x,y) \triangleq \mathscr{B}_{\mathscr{I}}(1,x,y)$ [8, 9]. Let us remark that $S \neq 0$ under hypothesis H_1 (target) and $S = 0$ under hypothesis H_0 (no target), thus the false alarm probability is:

$$\begin{aligned} P_{fa}^{CA-CFAR}(T) &\triangleq P(X_n/Z_n > T|H0) \\ &\triangleq P_d^{CA-CFAR}(T|S=0). \end{aligned}$$

The treshold T depends on N_n and L.

The CA-CFAR processor was studied in many different situations and it was shown that the CA-CFAR processor performances are degraded (excessive false alarm rate or target masking) when this processor is used in nonhomogeneous backgrounds [7].

In this communication, the hypothesis of a homogeneous background is removed and a new CFAR thresholding is introduced, allowing one to design new CFAR processors with other background estimators than the arithmetic mean. Finally, a new CFAR processor, named Q-CFAR, is introduced

[1] a false alarm is detecting a target when no target is present

that uses a background estimator adapted to nonhomogeneous backgrounds. Numerical experiments performed with nonhomogeneous backgrounds show that this new CFAR processor provides an improvement of the false alarm regulation.

2. GENERALIZED CFAR THRESHOLDING

In this section, a generalization of the CFAR thresholding to other background estimators is proposed.

Let us note $\widehat{m}_n$ the background estimate at the pixel n, then the generalized detection test is:

$$\frac{X_n}{\widehat{m}_n} \underset{H_0}{\overset{H_1}{\gtrless}} \tau. \tag{3}$$

The hypothesis performed with the generalized CFAR tresholding is that the estimate of the background is a gamma random variate with mean m_n and order $N_n^{eq}L$: $\widehat{m}_n \sim \mathscr{G}(m_n, N_n^{eq}L)$.

Thus the generalized CFAR thresholding (G-CFAR) only requires the knowledge of the two first moments of the background estimator pdf (probability density function). The parameter N_n^{eq} is the equivalent number of pixels such that the variance of our background estimator (in nonhomogeneous backgrounds) is equal to the variance of the arithmetic mean (in homogenous backgrounds). The determination of N_n^{eq} is described in sections 3.1 and 3.2.

Following [4], the performance of the generalized detection test (G-CFAR) can be obtained:

$$P_d^{G-CFAR}(\tau|S) \triangleq 1 - \mathscr{I}\left(\frac{\frac{\tau}{N_n^{eq}(1+S)}}{1+\frac{\tau}{N_n^{eq}(1+S)}}, L, N_n^{eq}L\right). \tag{4}$$

The false alarm probability is:

$$P_{fa}^{G-CFAR}(\tau) \triangleq P_d^{G-CFAR}(\tau|S=0). \tag{5}$$

The treshold τ depends on N_n^{eq} and L. Note that the expressions of the CA-CFAR processor are obtained if the background estimator considered is the arithmetic mean and the background is homogeneous: $N_n^{eq} = N_n$.

In the following section, the generalized CFAR thresholding is used to design a new CFAR processor adapted to nonhomogeneous situations.

3. BACKGROUND ESTIMATION

In this section, a background estimator is presented, characterized and used in order to design a new CFAR processor (Q-CFAR) thanks to the generalized CFAR thresholding presented in the previous section. The considered background estimator being adapted to gaussian noise, the logarithm of the data $\boldsymbol{Y} \triangleq \log[\boldsymbol{X}]$ is used in order to manage gamma noise. This operation transforms the multiplicative noise into additive noise and allows one to improve the performance with the background estimator even if the resultant noise is not strictly gaussian.

3.1 Background estimator

Firstly, it is assumed that the log-background $\boldsymbol{\mu} \triangleq E[\boldsymbol{Y}]$ evolves locally (in the region ω_n) as a polynomial of order lower or equal to 2, *i.e.* $\mu_k \triangleq a_n \times {i_k}^2 + b_n \times {j_k}^2 + c_n \times i_k \times j_k + d_n \times i_k + e_n \times j_k + f_n$, where a_n, b_n, c_n, d_n, e_n, f_n are the true parameters of the polynomial form.
For sake of simplicity, we denote $\boldsymbol{\mu}_{\omega_n} = \{\mu_k\}_{k\in\omega_n}$ ($\boldsymbol{\mu}_{\omega_n} \in \mathscr{R}^{N_n}$) the log-background values in ω_n. Let us introduce the true parameter vector $\boldsymbol{\theta}_n^0$:

$$\boldsymbol{\theta}_n^0 \triangleq [a_n, b_n, c_n, d_n, e_n, f_n]^T,$$

where $\boldsymbol{A}^T$ denotes the transpose of $\boldsymbol{A}$ and the $N_n \times 6$ matrix $\boldsymbol{M}_{\omega_n}$ such each line of $\boldsymbol{M}_{\omega_n}$ is given by:

$$\forall k \in \{1 \cdots N_n\},\ \boldsymbol{M}_{\omega_n}(k,:) \triangleq [{i_k}^2, {j_k}^2, i_k j_k, i_k, j_k, 1].$$

Then the log-background in ω_n is given in vector form by:

$$\boldsymbol{\mu}_{\omega_n} = \boldsymbol{M}_{\omega_n}\boldsymbol{\theta}_n^0.$$

Assuming that the vector $\boldsymbol{Y}_{\omega_n} = \{Y_p,\ p \in \omega_n\}$ is the addition of the vector $\boldsymbol{\mu}_{\omega_n}$ and a vector of independent and identically distributed gaussian noise realizations with variance σ^2 and zero mean, the maximum likelihood estimation for $\boldsymbol{\theta}_n^0$ is the minimizer of the following criterion:

$$J(\boldsymbol{\theta}_n) \triangleq (\boldsymbol{Y}_{\omega_n} - \boldsymbol{M}_{\omega_n}\boldsymbol{\theta}_n)^T (\boldsymbol{Y}_{\omega_n} - \boldsymbol{M}_{\omega_n}\boldsymbol{\theta}_n), \tag{6}$$

that reads:

$$\widehat{\boldsymbol{\theta}}_n = \left({\boldsymbol{M}_{\omega_n}}^T \boldsymbol{M}_{\omega_n}\right)^{-1} {\boldsymbol{M}_{\omega_n}}^T \boldsymbol{Y}_{\omega_n}.$$

It can be easily proved that this estimator is unbiased since:

$$\begin{aligned} E[\widehat{\boldsymbol{\mu}}_{\omega_n}] &= E\left[\boldsymbol{M}_{\omega_n}\left({\boldsymbol{M}_{\omega_n}}^T \boldsymbol{M}_{\omega_n}\right)^{-1} {\boldsymbol{M}_{\omega_n}}^T \boldsymbol{Y}_{\omega_n}\right] \\ &= E[\boldsymbol{Y}_{\omega_n}] = \boldsymbol{\mu}_{\omega_n}. \end{aligned}$$

Moreover the covariance matrix for $\widehat{\boldsymbol{\theta}}_n$ is given by:

$$\begin{aligned} cov(\widehat{\boldsymbol{\theta}}_n) &= E\left[\left(\widehat{\boldsymbol{\theta}}_n - \boldsymbol{\theta}_n^0\right)^2\right] \\ &= E\left[\left(\left({\boldsymbol{M}_{\omega_n}}^T \boldsymbol{M}_{\omega_n}\right)^{-1} {\boldsymbol{M}_{\omega_n}}^T (\boldsymbol{Y}_{\omega_n} - \boldsymbol{m}_{\omega_n})\right)^2\right] \\ &= \sigma^2 \left({\boldsymbol{M}_{\omega_n}}^T \boldsymbol{M}_{\omega_n}\right)^{-1}. \end{aligned}$$

Which leads to the covariance matrix for $\widehat{\boldsymbol{\mu}}_{\omega_n}$:

$$\begin{aligned} cov(\widehat{\boldsymbol{\mu}}_{\omega_n}) &= E\left[\left(\widehat{\boldsymbol{\mu}}_{\omega_n} - \boldsymbol{\mu}_{\omega_n}\right)^2\right] \\ &= E\left[\left(\boldsymbol{M}_{\omega_n}\widehat{\boldsymbol{\theta}}_n - \boldsymbol{M}_{\omega_n}\boldsymbol{\theta}_n^0\right)^2\right] \\ &= \boldsymbol{M}_{\omega_n} E\left[\left(\widehat{\boldsymbol{\theta}}_n - \boldsymbol{\theta}_n^0\right)^2\right] {\boldsymbol{M}_{\omega_n}}^T \\ &= \sigma^2 \boldsymbol{M}_{\omega_n}\left({\boldsymbol{M}_{\omega_n}}^T \boldsymbol{M}_{\omega_n}\right)^{-1} {\boldsymbol{M}_{\omega_n}}^T. \end{aligned}$$

Finally the estimation variance at the pixel under test n is given by:

$$var(\widehat{\mu}_n) = \sigma^2 \boldsymbol{v}_n \left({\boldsymbol{M}_{\omega_n}}^T \boldsymbol{M}_{\omega_n}\right)^{-1} {\boldsymbol{v}_n}^T, \tag{7}$$

where

$$\boldsymbol{v}_n = [{i_n}^2, {j_n}^2, i_n j_n, i_n, j_n, 1]^T.$$

3.2 Adaptation to gamma noise

The background estimator is used on the logarithm of the data $\log(\boldsymbol{X})$. Relations can be established between the values $\widehat{\mu}_n$ and $var(\widehat{\mu}_n)$ estimated from the logarithm of the data and the values $\widehat{m}_n$ and $var(\widehat{m}_n)$.

Let u be a gamma random variate with mean m and order L and $v = \log(u)$ then [9]:

$$E_u[v] = \psi(L) - \log(L/m), \tag{8}$$

$$var_u(v) = \zeta(2, L), \tag{9}$$

where $\psi(z) \triangleq \frac{d}{dz}\log[\Gamma(z)]$ is the Digamma function and $\zeta(s,\alpha) \triangleq \sum_{k=0}^{\infty} \frac{1}{(k+\alpha)^s}$ is the Hurwitz Zeta function [8, 9].

From equation 8, it can be established that:

$$\widehat{\mu}_n = \psi(L) - \log(L/\widehat{m}_n),$$

and then:

$$\widehat{m}_n = L\exp[\widehat{\mu}_n - \psi(L)].$$

From equation 9, the variance of the gaussian noise σ^2 is equal to $\zeta(2,L)$ and the estimation variance $\widehat{\mu}_n$ can be computed using equation 7.
The background estimate is assumed to be a gamma random variate with order $N_n^{eq}L$, which can be evaluated with equation 7 by inverting:

$$var(\widehat{\mu}_n) = \zeta(2, N_n^{eq}L)$$

In the following, the presented background estimator will be referred to as Q-CFAR background estimator. The Q-CFAR background estimator allows one to manage different kinds of nonhomogeneous backgrounds, *e.g.* constant, linear or quadratic log-backgrounds and more generally all log-backgrounds that is locally a function of differentiability class $\mathscr{C}^2$. Then the proposed detector is suit to more background models than the CA-CFAR (homogeneous backgrounds). In addition, the model used allows one a better false alarm regulation than the CA-CFAR (constant model) and good detection performance as it will be shown in the following experiments.

4. EXPERIMENTS

The experiments establish a comparison between the detection performance obtained with the CA-CFAR processor and the new Q-CFAR processor. At different locations in the image and for different expected false alarm probabilities, the detection probability and the false alarm probability of the processors are estimated by a Monte-Carlo method (10^6 realizations for the P_{fa} and 10^5 for the P_d) in order to be compared. Firstly, the data generation used in these experiments is defined, then the comparison of the detection performance is achieved.

4.1 Data generation

To generate the data $\boldsymbol{X}$, we first generate a background $\boldsymbol{m}$, the same background is kept for all the noise realizations.

The logarithm of the background $\boldsymbol{\mu}$ is a filtered gaussian noise with null mean and variance equal to 10. The filter used is a normalized gaussian filter with width 2.2 pixels. Then the background $\boldsymbol{m}$ is the exponential of $\boldsymbol{\mu}$: $\boldsymbol{m} = \exp(\boldsymbol{\mu})$.

For the detection probability study, targets are added to the background. For each realization, the data $\boldsymbol{X}$ are obtained by generating a gamma noise with order L and mean $\boldsymbol{m}$: $\boldsymbol{X} \sim G(\boldsymbol{m}, L)$. In the experiments, the order of the gamma noise is $L = 4$ and the target SNR is $S_{dB} = 7\,dB$ with $S_{dB} = 10\log_{10}(S)$.

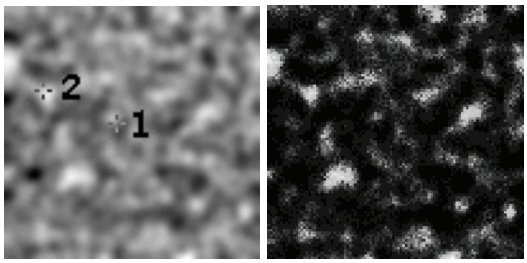

Figure 1: On the left, logarithm of the background $\boldsymbol{\mu}$ used for the experiments (100x100 pixels), the target positions are indicated by crosses. On the right, example of an image $\boldsymbol{X}$ (gamma correction of value 3 on the grey level scale for visualization).

In figure 1, the logarithm of the background $\boldsymbol{\mu}$ used for the experiments is presented, the target positions are indicated by crosses and a number identifies each target. In addition an example of generated data $\boldsymbol{X}$ is provided.

4.2 Detection performance comparison

Figures 2 and 5 present the comparisons of the detection performances obtained with the CA-CFAR processor and the proposed processor for the targets 1 and 2. The region ω_n is a square of 5x5 pixels for figure 2 (7x7 pixels for figure 5), centered on the pixel under test and the central pixel of the square is not included in the region ω_n. For comparison the theoretical detection performance of the ideal detector (*i.e.* the detector for which the background is known) is given.

In figure 2, the CA-CFAR processor does not respect the expected false alarm probability and has a poor detection probability. The Q-CFAR processor respects the expected false alarm probability and its detection probability curve is over the detection probability curve of the CA-CFAR processor. The Q-CFAR processor presents a detection loss compared with the ideal detector; this detection loss is due to the variance of the Q-CFAR background estimator. Indeed when the estimation variance decreases (N_n^{eq} increases), the detection probability increases and asymptotically tends towards the detection probability of the ideal detector (known background). To illustrate this phenomena, figure 3 is given in order to compare the detection probability obtained with the ideal detector and with the proposed technique for different sizes of the region ω_n ($L = 4$, $S_{dB} = 7\,dB$).

Moreover **on nonhomogeneous backgrounds**, the estimation variance of the Q-CFAR background estimator is higher than the estimation variance of a constant background estimator. As a consequence, for a homogeneous region ω_n, the CA-CFAR provides a better detection probability than the proposed detector. Figure 4 presents the ratio ρ between the detection probability of the proposed detector and the detection probability of the CA-CFAR computed for different sizes of the region ω_n and false alarm probabilities considering homogeneous backgrounds. Let us remark that $\rho \leq 1$ as

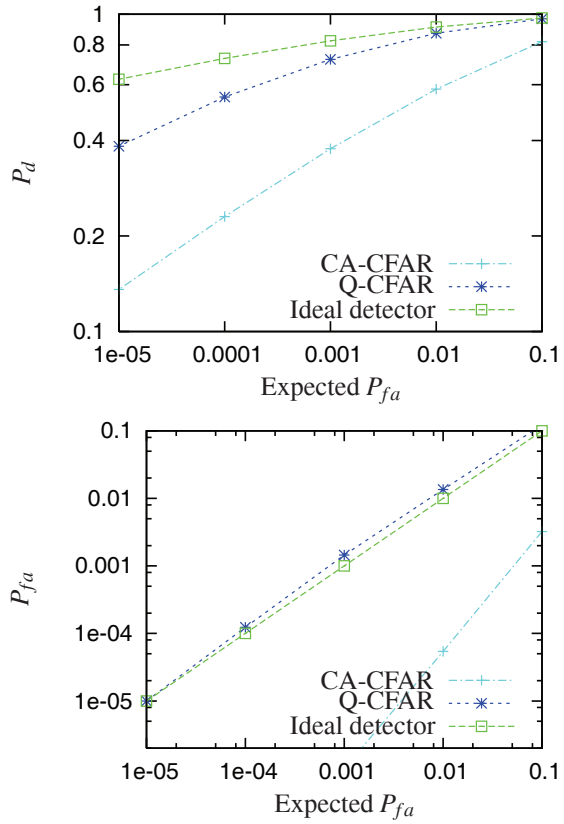

Figure 2: Comparison of the detection performances of the CA-CFAR processor and the proposed Q-CFAR processor for the target number 1. The region ω_n is a square of 5x5 pixels, the central pixel of the square is not included in the region ω_n.

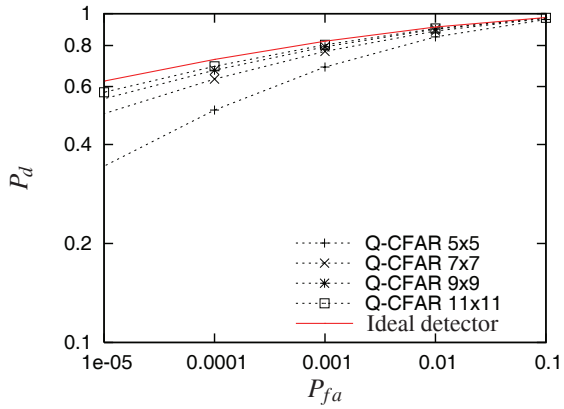

Figure 3: Comparison of the detection probability obtained with the ideal detector and with the proposed technique for different sizes of the region ω_n ($L = 4$, $S_{dB} = 7\,dB$).

the CA-CFAR is the optimal detector on homogeneous backgrounds [3]. The value of the ratio ρ is lower for the lowest false alarm probabilities than for the highest and increases as the region ω_n grows for a given false alarm probability. In addition, it can also be pointed out that the detection probability of the proposed detector for a region ω_n of size 9x9 (or greater) is relatively close to the detection probability of the CA-CFAR on homogeneous backgrounds.

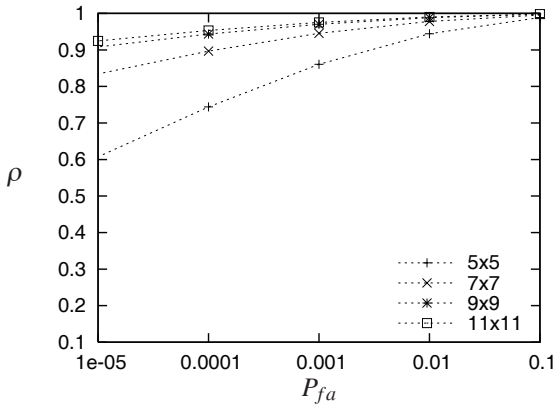

Figure 4: **On homogeneous backgrounds**, ratio ρ between the detection probability of the proposed detector and the detection probability of the CA-CFAR for different sizes of the region ω_n and for different false alarm probabilities ($L = 4$, $S_{dB} = 7\,dB$).

However, **on nonhomogeneous backgrounds** the proposed detector allows one an improved false alarm regulation compared to the CA-CFAR that can leads to better detection performance (see results obtained with target number 1). This improved false alarm regulation on nonhomogeneous backgrounds is the major contribution of the proposed detector.

In figure 5, the CA-CFAR processor has a high detection probability but does not respect the expected false alarm rate. The Q-CFAR processor is even CFAR and its detection probability curve is closer to the detection probability curve of the ideal detector than for target number 1 as the number of pixels N_n in ω_n has increased for this example ($N_n = 48$).

These experiments show the benefit of the proposed processor on the detection performance. In nonhomogeneous backgrounds, the expected false alarm probability can be respected with the proposed processor. Additionally, these experiments show that the generalized CFAR thresholding presented in this paper can be used to design new CFAR processors that use different background estimators from the arithmetic mean.

5. CONCLUSION

In this communication, a generalization of the CA-CFAR processor to nonhomogeneous gamma-distributed backgrounds has been proposed. The generalized CFAR thresholding introduced allows one to use other background estimators from the arithmetic mean.

An example of application has been provided by the design of a new Q-CFAR processor with a background estimator adapted to nonhomogeneous backgrounds. Then, experiments show the benefit of the proposed processor com-

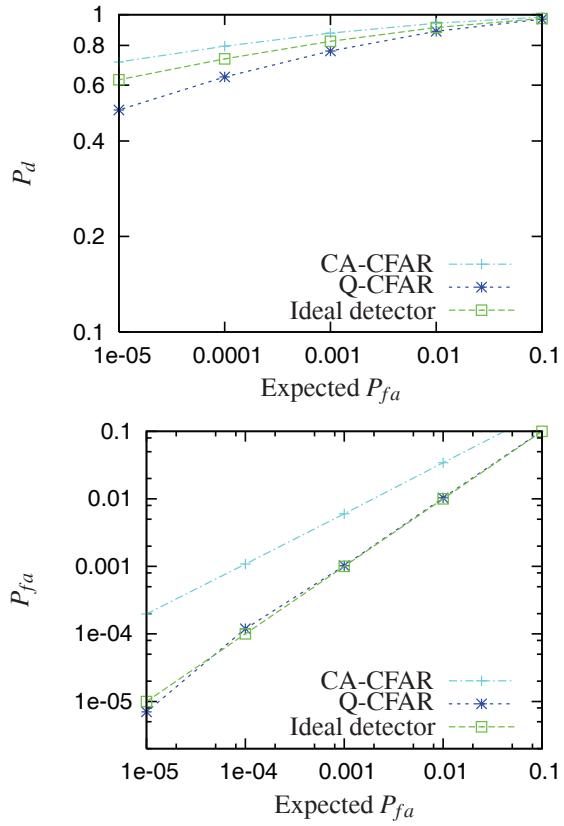

Figure 5: Comparison of the detection performances of the CA-CFAR processor and the proposed Q-CFAR processor for the target number 2. The region ω_n is a square of 7x7 pixels, the central pixel of the square is not included in the region ω_n.

pared to the CA-CFAR processor. The proposed processor provides a better false alarm regulation in nonhomogeneous backgrounds.

The main advantage of the generalized CFAR thresholding is to divide the detection problem into a background estimation problem and a CFAR thresholding problem. In future works, a study of the limits of the proposed CFAR thresholding, and more particularly, the hypothesis on the background estimate probability density function (see section 2), will be investigated. Finally, it seems interesting to develop more accurate estimation method with a lower estimation variance to obtain better detection probability.

6. ACKNOWLEDGEMENTS

The authors thank the Délégation Générale de l'Armement (DGA) and the Centre National pour la Recherche Scientifique (CNRS) for supporting the Ph.D. thesis of Éric Magraner. The authors would thank more particularly Sébastien Paillardon of the DGA.

REFERENCES

[1] P. Swerling, "Detection of RADAR Echoes in Noise Revisited", *IEEE Trans. on Information Theory*, vol. 12, N 3, pp. 348–361, Jul. 1966.

[2] H. M. Finn and P. S. Johnson, "Adaptive Detection Mode With Threshold Control As a Function of Spatially Sampled Clutter Estimation", *RCA Review*, vol. 29, N 3, pp. 414–464, 1968.

[3] P. P. Gandhi and S. A. Kassam, "Optimality of the Cell Averaging CFAR Detector", *IEEE Trans. on Information Theory*, vol. 40, N 4, Jul. 1994.

[4] C. Alberola-López and J. R. Casar-Corredera and G. de Miguel-Vela, "Object CFAR Detection in Gamma-Distributed Textured-Background Images", *IEE Proc. Vision, Signal and Image Processing*, vol. 146, N 3, pp. 130–136, Jun. 1999.

[5] H. L. Van Trees, *Detection, Estimation, and Modulation Theory - Part I. Detection, Estimation, and Linear Modulation Theory*, Wiley-Interscience, George Mason University, 2001.

[6] A. Papoulis, *Probability, Random Variables, and Stochastic Processes - Third Edition*, WCB Mc Graw-Hill, Polytechnic University, 1991.

[7] P. P. Gandhi and S. A. Kassam, "Analysis of CFAR Processors in Nonhomogeneous Background", *IEEE Trans. Aerospace and Electronic Systems*, vol. 24, N 4, Jul. 1988.

[8] M. Abramowitz and I. Stegun, *Handbook of mathematical functions with formulas, graphs, and mathematical tables*, Dover Publications, New York, 1972.

[9] I. S. Gradshteyn and I. M. Ryzhik, *Table of Integrals Series and Products, Sixth Edition*, Academic Press, New York, 2000.